

# LLMs for Agentic Home Energy Management

Sokipriala Jonah

Centre for Computational Science and Mathematical Modelling  
Coventry University  
Coventry, United Kingdom

**Abstract**—Home Energy Management Systems (HEMS) can reduce residential electricity costs and support demand response, but adoption is limited by the difficulty of translating household preferences into technical scheduling constraints. This paper evaluates whether large language model (LLM) agents can provide a practical natural-language interface for multi-appliance home energy scheduling. We present a tool-calling ReAct agent that uses live half-hourly Octopus Agile prices, weather forecasts, photovoltaic generation estimates, household usage data, and a retrieval-augmented knowledge base to schedule flexible loads against a mixed-integer linear programming (MILP) ground truth. Three commercial models, GPT-4o-mini, Gemini 2.5 Flash, and Claude Sonnet 4.6, are benchmarked across tariff days, constraint-conflict scenarios, weather-aware solar co-optimization, and week-long deployment. With native function calling, all models achieve 100% scheduling success and near-MILP optimality, while text-parsed action interfaces sharply reduce reliability. Constraint testing shows that cost-optimal and safety-optimal models differ: Claude is strongest under infeasibility and power-cap conflicts, while GPT-4o-mini is most efficient. Over a simulated week, agents capture 96.7–98.0% of oracle savings, projecting approximately £1,270 annual savings over an off-peak timer baseline. Code and a live demonstration are available at <https://github.com/sokistar24/ecohome-energy-agent> and <https://www.ecohomeagent.com/>.

**Index Terms**—Agentic AI, home energy management systems, large language models, demand response, load scheduling, solar self-consumption, dynamic retail tariffs, LLM benchmarking.

## I. INTRODUCTION

THE decarbonization of electricity systems requires rising shares of variable renewable generation to be integrated while maintaining reliable and affordable supply. This creates a growing need for demand-side flexibility [1], [2]. The International Energy Agency projects that global demand-response capacity must grow roughly tenfold between 2020 and 2030, with buildings and residential electric vehicles (EVs) contributing much of this potential [3], [4], [5]. The residential sector is especially attractive because flexible loads, including EV charging, wet appliances, heating, and cooling, can often be shifted in time without materially affecting the service delivered to occupants [6], [7].

Home Energy Management Systems (HEMS) are intended to realize this flexibility by scheduling household devices against price and generation signals. Although HEMS have demonstrated cost reductions and demand-response value, deployment remains below the level required for decarbonization targets [3], [8]. A key barrier is the user-interaction burden: conventional HEMS require households to translate everyday preferences into technical parameters, which discourages adoption among non-expert users [9], [10].

Large language models (LLMs) offer a possible route around this barrier. Modern LLMs can follow task instructions without example demonstrations [11], [12], [13], invoke external tools, and, when organized as agents that interleave reasoning with actions [14], [15], decompose a natural language request into data retrieval, analysis, and control decisions. Beyond reducing the parameterization burden, a conversational agent can explain its recommendations, answer ad hoc questions about consumption and tariffs, and ground its advice in a curated knowledge base of energy-saving practice through retrieval-augmented generation (RAG).

A small but growing body of work has begun to apply LLMs to home energy management, including conversational energy advice, natural-language interfaces to optimizers or model-predictive controllers, and autonomous scheduling agents [16], [17], [18], [19], [20]. Most of these systems use the LLM primarily as an interface layer: the model interprets a user request, provides advice, or extracts parameters that are then passed to a conventional controller or optimizer. The strongest move toward autonomous LLM-based scheduling is the agentic HEMS of El Makroum *et al.* [17], where an LLM orchestrator delegates to per-appliance specialist agents and commits schedules for a washing machine, dishwasher, and EV charger against Austrian day-ahead wholesale prices.

Benchmarked against MILP optima, that system achieved perfect multi-appliance coordination with Llama-3.3-70B. However, two other open-source models, Qwen-3-32B and GPT-OSS-120B, failed to coordinate all appliances despite perfect single-appliance performance. The study also reported that all models required explicit prompt guidance to answer analytical price queries. These results establish the feasibility of LLM-based HEMS orchestration, but they also expose four open questions that motivate the present paper:

- 1) **Model coverage.** Existing autonomous scheduling results are limited to open-source models. Since prior work explicitly suggests that stronger commercial models may improve orchestration [17], it remains unclear whether reported coordination failures are intrinsic to LLM-based scheduling or specific to the models and action interfaces tested.
- 2) **Price-only optimization.** Existing autonomous scheduling is based on day-ahead wholesale prices alone. For households with rooftop PV, the relevant objective is net cost after solar self-consumption, which requires weather-aware PV forecasting and changes the structure of the optimal schedule.
- 3) **Single-day evaluation.** Prior autonomous HEMS evaluation uses a single price day and does not provide

statistical treatment. Robustness across price-volatility regimes therefore remains untested.

- 4) **Untested constraint conflicts.** Existing evaluations do not observe cases where the cost-optimal schedule violates a user constraint. As a result, agent behaviour under deadline, calendar, or household power-cap conflicts remains a safety-relevant blind spot.

We address these gaps with an agentic HEMS that improves both data grounding and evaluation rigor. The system is designed to operate on retail market data, specifically the half-hourly Octopus Energy Agile tariff in Great Britain, which exposes households to wholesale price volatility including negative-price events. It also uses weather forecasts to estimate on-site PV generation and optimize net electricity cost after solar self-consumption. Architecturally, we use a single tool-calling ReAct agent with native function calling rather than a hierarchical multi-agent design. This allows us to test whether stronger commercial models with structured tool interfaces can remove the need for the manual task decomposition used in earlier open-source deployments.

### A. Contributions

This paper makes three contributions:

- **C1 (Multi-day model benchmark).** We provide a statistically grounded comparison of commercial models from three providers, namely GPT-4o-mini, Gemini 2.5 Flash, and Claude Sonnet 4.6, for agentic multi-appliance HEMS scheduling. The models are evaluated over 12 distinct Agile tariff days spanning low-, medium-, and high-volatility regimes, with MILP ground truth, native function-calling versus text-parsed action interfaces, and analysis of cost, latency, and optimality. The benchmark culminates in a week-long rolling deployment simulation with statistically projected four-week costs, compared against MILP oracles and rule-based baselines.
- **C2 (Constraint-conflict stress suite).** We introduce a reusable adversarial scenario suite in which cost minimization conflicts with deadlines, appliance windows compete under a household power cap, calendar constraints are irregular or infeasible, and tools fail mid-run. We evaluate deadline-satisfaction rate, constraint-violation rate, feasibility cost premium, and failure modes derived from agent traces.
- **C3 (Weather-aware solar co-optimization).** We extend the agentic scheduling objective from price-only cost to net cost with PV self-consumption, using live forecast tooling and an irradiance-to-generation model. The resulting schedules are benchmarked against an extended MILP formulation that no longer decomposes per appliance, and are further analyzed for sensitivity to forecast error.

### B. Paper Structure

Section II reviews related work. Section III presents the system architecture. Section IV formalizes the scheduling problem, the extended MILP ground truth, and the evaluation metrics. Section V details the experimental design. Section VI reports the results. Section VII discusses implications and limitations. Section VIII concludes the paper.

## II. RELATED WORK

### A. LLM Agents and Agentic AI

Recent taxonomies distinguish single-purpose AI *agents* from *agentic AI* systems, in which an LLM acts as an autonomous reasoning engine that decomposes objectives, selects tools, and coordinates multi-step workflows without relying on predefined pipelines [21], [22], [23]. Hierarchical reasoning, adaptability, and tool-mediated decision-making are commonly identified as the capabilities that separate agentic systems from conventional automation [24]. The dominant implementation pattern is ReAct [14], [25], [26], which interleaves reasoning steps with tool invocations and observations, thereby producing inspectable traces that support debugging, validation, and failure analysis.

This capability is particularly relevant for HEMS. Since capable LLMs can operate without example demonstrations [11], [27], [28], agentic systems can be specified through task instructions and tool descriptions alone. This matters in residential energy management because household users cannot be expected to provide example scheduling requests or encode their preferences as technical constraints. A further practical advance is *native function calling*, where commercial model APIs return structured tool calls directly instead of relying on brittle parsing of free-form action strings. Whether this interface difference materially improves orchestration reliability in energy applications remains untested. Experiment 1 measures this effect directly.

### B. LLMs in Energy System Applications

Surveys of LLMs in the electricity sector identify domain adaptation, including retrieval augmentation, tool grounding, and fine-tuning, as important prerequisites for reliable deployment [29], [30], [27], [28]. Existing applications span several roles. As *code generators*, LLMs have produced optimization formulations for EV charging and demand-side management [31], [32], [33], [34]. As *diagnostic assistants*, customized models have routed tasks and retrieved domain knowledge for building operation and maintenance, outperforming general models on fault diagnosis [35]. As *controllers*, an agentic HVAC system deployed in operating offices achieved energy savings and comfort improvements, although in a single commercial building rather than a residential multi-appliance setting [36]. As *decision evaluators*, LLMs have recommended residential retrofits with high top- $k$  accuracy, but with limited contextual reasoning [37].

In smart-home applications, LLMs have generated Home-Assistant automation rules from natural language [38], [39], been combined with digital-twin context for general energy-saving actions [40], provided conversational energy advice without direct device control [41], interpreted user commands for a model-predictive controller that performs battery scheduling [42], and extracted scheduling parameters from dialogue for a conventional optimizer [10]. Across these systems, the LLM usually acts as an interface, assistant, or preprocessing layer in front of a traditional decision-making component, rather than as the entity that directly commits schedules.

### C. Agentic HEMS and Positioning of This Work

El Makroum *et al.* [17] move beyond the interface-only role by allowing an LLM orchestrator to make and commit scheduling decisions. Their system delegates to specialist appliance agents and matches MILP-optimal schedules with Llama-3.3-70B on Austrian day-ahead prices. This demonstrates that LLM-based HEMS orchestration is feasible, but four limitations define the departure point for our work.

First, the model coverage is limited to open-source checkpoints, two of which fail multi-appliance coordination. It remains unclear whether these failures reflect an inherent limitation of LLM orchestration or the specific capability level and action interface of the tested models. Second, the optimization signal is one-dimensional: scheduling is based on wholesale price only, with no weather input, on-site generation, or self-consumption objective. This omits a central requirement for PV-equipped households, which are a natural constituency for HEMS. Third, the evaluation uses a single day of prices, leaving robustness across price-volatility regimes untested. Fourth, the reported scenarios do not create cases where the cost optimum violates a user constraint, so constraint-conflict behaviour is not observed. A further methodological gap is that, as in much of the current literature, the reported success rates are not accompanied by statistical testing.

This paper addresses these gaps by evaluating commercial function-calling models over multiple tariff regimes, extending the objective to weather-aware PV self-consumption, introducing explicit constraint-conflict stress tests, and benchmarking sustained deployment against MILP oracles and rule-based household baselines. Table I summarizes the positioning.

## III. SYSTEM ARCHITECTURE

### A. Overview

Fig. 1 shows the proposed system. A single LLM-based agent, implemented using the LangGraph ReAct construction, receives a natural language request such as “When should I charge my EV tomorrow to minimise cost?”. It then follows a reason and act loop: it selects a tool, observes the result, and repeats this process until it can commit a schedule and produce a recommendation. The system prompt defines the agent’s role as an energy advisor, specifies the workflow it should follow, and sets the expected recommendation format. In particular, the agent is instructed to retrieve prices and weather before recommending a schedule, ground advice in retrieved energy-saving tips, and quantify the expected savings. Temperature is fixed at 0 for reproducibility.

Unlike the hierarchical orchestrator and specialist-agent design of [17], all coordination in this system is handled by one agent. This deliberately minimal design allows Experiment 1 to test whether commercial models with native function calling can sustain multi-appliance coordination without manual task decomposition.

### B. Tool Layer

The agent has access to the following six tools, which together define its complete action space for the scheduling task:

- **Electricity price retrieval** returns half-hourly import prices from the Octopus Energy Agile tariff [43], measured in GBP/kWh over 48 daily slots, for a specified date. Agile passes day-ahead wholesale market dynamics through to a retail tariff, including occasional negative prices. Since prices are published before the delivery day, Agile provides a realistic and reproducible dynamic-pricing signal for GB households.
- **Weather forecast retrieval** returns hourly forecasts for temperature, cloud cover, and global horizontal irradiance from Open-Meteo [44] for the household location and a specified date.
- **PV generation prediction** converts forecast irradiance and temperature into 48 half-hourly slots of expected PV output using the model in Sec. V-D1.
- **Cheapest-window computation** returns the cheapest and most expensive candidate start-slot windows for a given run length, factoring out slot arithmetic that would otherwise consume reasoning tokens.
- **Appliance scheduling** commits an appliance’s start slot for a specified date after validating that it fits within the horizon. This is the only tool whose invocation the scorer treats as a scheduling decision; prose recommendations are not executed.
- **Infeasibility reporting** formally records that a request cannot be satisfied under the stated constraints. The correct behaviour on the S4 scenarios of Sec. V-C is to invoke this tool rather than commit a schedule that violates a constraint.

Experiment 1 uses a price-only subset with **Weather forecast retrieval** and **PV generation prediction** removed, so that comparison against the price-only MILP is apples-to-apples; all other experiments use the full six-tool set. The deployed web system additionally provides RAG-based advisory retrieval, a household usage database, and a savings calculator; these are documented in Appendix D and are not exercised by any experiment.

### C. Model Backends and Action Interfaces

The agent is model-agnostic. We evaluate three commercial models, one per provider: GPT-4o-mini from OpenAI, Gemini 2.5 Flash from Google, and Claude Sonnet 4.6 from Anthropic. These models occupy broadly comparable price and latency tiers, so cross-model differences are interpreted as model and interface effects rather than tier effects (Table II). Any model slot can be replaced by that provider’s frontier tier without changing the evaluation harness, although that extension is left contingent on budget.

Open-source models are not re-run locally. Instead, comparisons to open-source systems are made against the results reported in [17], clearly labelled as literature values obtained under a different market and architecture. All commercial models are accessed using pinned model identifiers recorded for each run, since provider-side updates can otherwise weaken reproducibility. Two action interfaces are compared where supported: native function calling, where the API returns structured tool invocations, and text-parsed ReAct actions,

TABLE I  
POSITIONING RELATIVE TO CLOSELY RELATED LLM-BASED RESIDENTIAL ENERGY SYSTEMS

Work	LLM role / models	Weather / PV	Eval. horizon	Constraint conflicts	Objective / data
Michelon <i>et al.</i> [10]	Parameter extraction for external optimizer	No	N/A	No	Optimizer cost; dialogue evaluation
Raghavan & Giridhar [42]	Natural-language interface to MPC using Phi-3 Mini	No	N/A	No	Battery cost via MPC solver
Gkalinikis <i>et al.</i> [41]; Yang <i>et al.</i> [20]; Jung <i>et al.</i> [16]	Conversational energy advisor or recommendation system without direct device control	No	N/A	No	Advice quality, user interaction, or recommendation quality
El Makroum <i>et al.</i> [17]	Autonomous orchestrator using three open-source models	No, prices only	1 day, 75 runs	Not tested	Electricity cost using ENTSO-E wholesale prices
<b>This work</b>	<b>Autonomous single tool-calling agent using commercial LLMs</b>	<b>Yes, live forecast and PV model</b>	<b>12 days, 1,100+ runs, significance tests</b>	<b>Dedicated stress suite</b>	<b>Net cost with self-consumption using live Octopus Agile retail tariff</b>

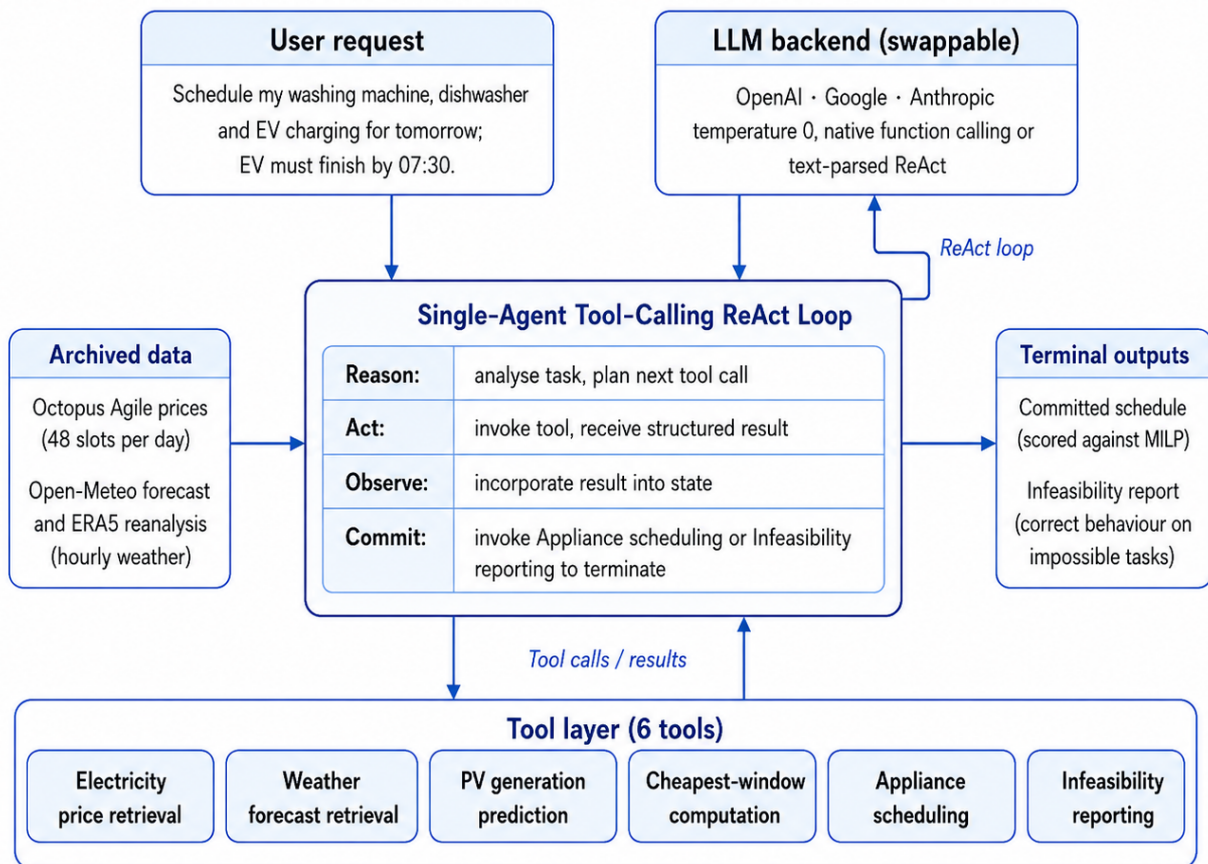


Fig. 1. System architecture. A LangGraph ReAct agent reasons over a tool layer spanning live external APIs, including the Octopus Energy Agile tariff and Open-Meteo weather, a household SQLite database of usage and solar generation, a Chroma vector store of energy-saving documents for RAG, and analytical utilities. The agent iterates through tool use and observation until it commits a schedule and returns a recommendation.

TABLE II  
EVALUATED LLM BACKENDS

Model	Provider	Function calling	Model identifier
GPT-4o-mini	OpenAI	Yes	gpt-4o-mini
Gemini 2.5 Flash	Google	Yes	gemini-2.5-flash
Claude Sonnet 4.6	Anthropic	Yes	claude-sonnet-4-6

where tool calls are extracted from free-form model output. Holding the agent, tools, and prompts fixed across models isolates the model and interface as the main experimental variables.

#### D. Temporal Grounding

LLMs do not share a consistent notion of “now”. Some backends are given the real-world date at inference time, while others infer it from tool outputs or training priors. As a result, a relative request such as “tomorrow” can resolve to different calendar days across models. We observed this directly during development, when the agent anchored “today” to the seeding date of the sample database rather than the wall-clock date.

All evaluations therefore pin time explicitly. Each run declares the evaluation date and time, all tools resolve relative dates against that declared date rather than the system clock, and archived price and weather data are keyed to it. This ensures that every model faces the same reproducible temporal frame.

#### E. Security and Scope Guarding

User inputs pass pre-LLM validation before reaching the agent. This includes length limits, malformed-input rejection, and pattern-based screening for prompt-injection attempts [45]. The system prompt also restricts the agent to the home-energy domain. These measures follow the defence-in-depth approach of [17]. All experiments in this paper use valid in-domain requests, and adversarial red-teaming is outside the scope of the evaluation.

## IV. PROBLEM FORMULATION

### A. Notation and Setting

Time is discretized into  $T=48$  half-hourly slots  $t \in \{0, \dots, 47\}$  of length  $\Delta = 0.5$  h, matching the Agile tariff settlement period. Each slot has an import price  $C_t$  in GBP/kWh and an export price  $F_t$  in GBP/kWh. We use a flat export price  $F_t \equiv F$ , with  $F = 5$  p/kWh, representing a typical standalone Smart Export Guarantee rate. Under Agile,  $C_t$  may become negative during high-renewable periods, so the ground-truth formulation must handle both positive and negative import prices, as detailed in Appendix A.

Forecast PV generation in slot  $t$  is denoted by  $\hat{G}_t$  in kWh, and the inflexible household base load is denoted by  $B_t$  in kWh. The base load is estimated from household usage history. Each schedulable appliance  $a \in A$  has rated power  $P_a$  in kW, duration  $d_a$  in half-hourly slots, and latest permissible start time  $t_{\max,a}$ . The binary decision variable  $x_{a,t}$  equals 1

TABLE III  
APPLIANCE SPECIFICATIONS AT HALF-HOURLY RESOLUTION

Appliance	Power (kW)	Duration (min)	Slots
Washing machine	2.0	120	4
Dishwasher	1.8	90	3
EV charger	7.4	360	12

if appliance  $a$  starts in slot  $t$ , and 0 otherwise. The derived running-state variable

$$u_{a,t} = \sum_{k=\max(0, t-d_a+1)}^t x_{a,k}$$

indicates whether appliance  $a$  is operating in slot  $t$ . Appliance specifications are shown in Table III, following [17] and re-expressed at half-hourly resolution.

### B. Net-Cost Objective with PV Self-Consumption

The scheduled flexible load in slot  $t$  is

$$L_t = \sum_{a \in A} P_a \Delta u_{a,t}.$$

The household’s net electricity cost over the day is then

$$J = \sum_{t=0}^{T-1} \left[ C_t (L_t + B_t - \hat{G}_t)^+ - F (\hat{G}_t - L_t - B_t)^+ \right], \quad (1)$$

where  $(\cdot)^+ = \max(\cdot, 0)$ . The first term represents energy imported from the grid when household demand exceeds on-site PV generation. The second term represents revenue from exporting surplus PV generation. Setting  $\hat{G}_t \equiv 0$  and  $B_t \equiv 0$  recovers the price-only objective used in [17], which we use as a baseline in Experiment 3.

When  $C_t > F$ , shifting flexible load into PV-surplus periods reduces imports valued at  $C_t$  and avoids exporting the same energy at the lower rate  $F$ . This creates the self-consumption incentive that price-only scheduling ignores. When Agile import prices become negative, however, the relationship can reverse, since importing from the grid may be economically preferable to consuming on-site PV. This makes the weather-aware scheduling problem richer than a simple self-consumption maximization task. No battery is modelled in this study; storage is left for future work.

### C. Constraints and Extended MILP Ground Truth

Ground-truth schedules minimize (1) subject to the following constraints:

$$\sum_{t=0}^{t_{\max,a}} x_{a,t} = 1, \quad \forall a \in A, \quad (2)$$

$$x_{a,t} = 0, \quad \forall a \in A, t > T - d_a, \quad (3)$$

$$t + d_a \leq t_a^{\text{cal}} - \beta \quad \text{if } x_{a,t} = 1, \quad \forall a \in A_{\text{ddl}}, \quad (4)$$

$$\sum_{a \in A} P_a u_{a,t} \leq P^{\text{cap}}, \quad \forall t. \quad (5)$$

Constraint (2) requires each appliance to be scheduled exactly once within its permissible start window. Constraint (3) prevents schedules that would extend beyond the daily horizon. Constraint (4) enforces calendar-derived deadlines for appliances in  $A_{ddl}$ , such as the EV in the standard setting, with  $\beta$  representing a user-defined buffer. Constraint (5) enforces the household power cap  $P^{cap}$ .

Two features distinguish this formulation from the price-only case. First, the shared PV resource in (1) couples the scheduling decisions of all appliances. Second, the power-cap constraint (5) prevents appliances from being optimized independently when their operating windows overlap. The resulting problem therefore no longer decomposes into separate per-appliance searches, unlike the price-only setting in [17].

We linearize the positive-part terms using import and export variables and solve the resulting mixed-integer linear program using PuLP 3.3 with the CBC backend. Each instance solves in well under one second. The full formulation, including the binary complementarity treatment required when Agile prices satisfy  $C_t < F$ , is given in Appendix A.

#### D. Evaluation Metrics

- **Success rate:** the fraction of runs in which all requested appliances are scheduled and committed.
- **Optimality rate:** the fraction of runs in which the committed schedule attains the MILP optimum. For sub-optimal schedules, the cost gap is

$$\gamma = \frac{J_{\text{agent}} - J^*}{|J^*|},$$

where  $J_{\text{agent}}$  is the agent’s realised cost and  $J^*$  is the MILP optimum.

- **Self-consumption ratio:** the share of realised PV generation consumed on site,

$$\text{SCR} = \frac{\sum_t \min(L_t + B_t, G_t)}{\sum_t G_t},$$

evaluated using realised generation  $G_t$  in Experiment 3.

- **Deadline-satisfaction rate:** the fraction of runs in which all calendar and deadline constraints are satisfied.
- **Constraint-violation rate:** the fraction of runs in which the agent commits a schedule that violates at least one hard constraint.
- **Feasibility cost premium:** the additional cost accepted to satisfy constraints, relative to the unconstrained cost optimum. This is compared with the premium paid by the MILP itself in Experiment 2.
- **Infeasibility-reporting rate:** the fraction of provably infeasible scenarios in which the agent correctly reports infeasibility rather than committing a violating schedule.
- **Efficiency:** the number of ReAct iterations, token usage, wall-clock latency, and monetary cost per successful schedule, computed from provider token prices.

## V. EXPERIMENTAL DESIGN

### A. Model Funnel, Champion Selection, and Baselines

Commercial inference is metered, so model calls are allocated to the experiments needed to support each claim. All

three models are evaluated in Experiments 1, 2, and 3, and in the rolling deployment simulation of Experiment 4a. The forecast-noise sweep in Experiment 3 and the weekly joint-planning task in Experiment 4b are run only on a single champion model.

The champion is selected using a rule fixed before collecting results. The primary criterion is the product of multi-appliance success rate and optimality rate in Experiment 1. If models tie, the first tie-breaker is guided-prompt deadline satisfaction plus infeasibility-reporting rate in Experiment 2. The final tie-breaker is monetary cost per successful schedule.

Alongside the MILP oracle, all experiments include rule-based baselines computed at zero inference cost over the same archived data. These baselines represent common household scheduling strategies: a static off-peak timer that starts all flexible loads at 00:00 with the EV first, an immediate-start policy that runs loads on request, and a greedy cheapest-single-slot heuristic that ignores deadlines and the household power cap. The gap between these baselines and the MILP oracle defines the available savings. Each policy is reported as the share of that gap it captures.

### B. Experiment 1: Multi-Day Model Benchmark

**Hypothesis H1.** Commercial API models achieve reliable multi-appliance coordination, closing the gap reported for open-source models in [17], and native function calling improves reliability over text-parsed actions.

**Protocol.** Each model schedules a single appliance and all three appliances simultaneously across  $D = 12$  distinct Agile tariff days. The days are drawn from an Agile price archive covering 2026-04-20 to 2026-06-20 and stratified into low-, medium-, and high-volatility terciles using the coefficient of variation of  $C_t$ . Days containing negative-price slots are retained and flagged. Each model, day, and scenario cell is repeated  $R = 3$  times at temperature 0. Where supported, models are evaluated using both native function calling and text-parsed ReAct actions. Archived prices are fixed for each evaluation day so that all models face identical inputs.

**Analysis.** Success and optimality proportions are compared using Fisher’s exact test, with pairwise comparisons against the strongest baseline and Holm–Bonferroni correction. Nonzero cost gaps are compared using the Mann–Whitney  $U$  test. Efficiency metrics are reported as mean  $\pm$  standard deviation. The headline synthesis is a Pareto analysis over optimality rate, latency, and monetary cost per successful schedule.

### C. Experiment 2: Constraint-Conflict Stress Testing

**Hypothesis H2.** When cost optimality and hard constraints conflict, models differ systematically in how they prioritize constraints, and explicit conflict-resolution guidance improves reliable deadline satisfaction.

**Scenario suite.** Six scenario families are instantiated on real Agile days selected, or minimally edited with edits documented, so that the relevant conflict provably binds. The full scenario matrix is given in Appendix B.

**S1** tests deadline conflict: the globally cheapest EV charging window violates the calendar deadline, while the cheapest

feasible window costs  $\delta \in \{5, 10, 25, 50\}\%$  more. This sweeps the price of constraint compliance.

**S2** tests power-cap conflict: appliance cost optima overlap under a household cap of  $P^{\text{cap}} = 9\text{kW}$ . Since the EV charger alone draws 7.4kW, it cannot run concurrently with another appliance, forcing serialization.

**S3** tests irregular calendar interpretation, including a night-shift pattern, multiple candidate deadline events, and an event whose end time rather than start time defines the relevant constraint window.

**S4** tests infeasibility: no feasible window of length  $d_a$  exists before the calendar deadline  $t_a^{\text{cal}}$ . The correct behaviour is to report infeasibility rather than fabricate a schedule or silently relax the constraint.

**S5** tests instruction conflict: the user’s stated instruction, such as “charge overnight”, conflicts with a binding calendar constraint such as an early-morning departure.

**S6** tests tool-failure recovery by injecting a price API error on the first call and measuring whether the model retries successfully.

Each scenario is run under two prompts: a baseline prompt and a guided prompt containing explicit conflict-resolution rules. The guided prompt states that hard constraints dominate cost and that infeasible cases should be reported rather than violated, following the progressive guidance methodology of [17].

**Metrics.** We report deadline-satisfaction rate, constraint-violation rate, feasibility cost premium relative to the MILP premium, infeasibility-reporting rate for S4, recovery rate for S6, and a qualitative failure-mode taxonomy derived from event traces. Failure modes are assigned deterministically by the scorer. The conversational short-circuiting pattern reported in Section VI-A was verified by inspecting all 32 failing Claude single-appliance traces, each of which contained zero tool calls and a prose confirmation.

#### D. Experiment 3: Weather-Aware Solar Co-Optimization

**Hypothesis H3.** Co-optimizing against forecast PV generation reduces realized net cost and increases self-consumption relative to price-only scheduling, with graceful degradation under realistic forecast error.

1) *PV Forecast Model:* Forecast global horizontal irradiance  $I_t$  in  $\text{W/m}^2$  and ambient temperature  $T_t^{\text{amb}}$  from OpenMeteo are mapped to expected PV generation as

$$\hat{G}_t = P_{\text{stc}} \cdot \frac{I_t}{1000} \cdot [1 - \alpha(T_t^{\text{cell}} - 25)] \cdot \text{PR} \cdot \Delta, \quad (6)$$

where  $P_{\text{stc}} = 4.0\text{kWp}$  is the nameplate capacity,  $\alpha = 0.004\text{K}^{-1}$  is the temperature coefficient,  $\text{PR} = 0.80$  is the performance ratio, and  $\Delta = 0.5\text{h}$  is the slot length. Cell temperature is estimated using the NOCT approximation,

$$T_t^{\text{cell}} = T_t^{\text{amb}} + I_t(\text{NOCT} - 20)/800,$$

with  $\text{NOCT} = 45^\circ\text{C}$ .

2) *Protocol:* For each of  $D_w = 15$  evaluation days, stratified by forecast regime as sunny, mixed, or overcast using the forecast clear-sky index, each model schedules all three appliances under two objectives. The first is the price-only objective, where  $\hat{G}_t$  is withheld from the agent. The second is the net-cost objective, where weather and PV tools are enabled. Both policies are scored against realized generation and compared with the extended MILP.

Forecast-error sensitivity is assessed by perturbing  $\hat{G}_t$  with multiplicative noise at  $\pm 10\%$ ,  $\pm 25\%$ , and  $\pm 50\%$ . We report the resulting degradation in realized net cost and self-consumption ratio for each noise level and regime. The forecast-noise sweep is run only on the champion model.

#### E. Experiment 4: Longitudinal Deployment and Weekly Planning

**Hypothesis H4.** Over sustained operation, the champion agent captures most of the savings available to a per-day MILP oracle, strictly dominates rule-based scheduling, and extends its coordination ability from daily scheduling to joint weekly planning.

Because the Agile tariff is published only one day ahead, neither the agent nor the optimizer can observe prices beyond the next delivery day. Longer-duration evaluation is therefore operationalized in two information-honest ways.

1) *4a: Week-Long Rolling Deployment Simulation with Projected Four-Week Costs:* Over 7 consecutive archived days spanning both weekdays and a weekend, each model is invoked once per evening using that day’s published prices and weather forecast. It then commits the next day’s schedule. Committed schedules are scored on realized data, and costs accumulate across the week. Cumulative realized net cost is compared against the per-day extended MILP oracle, the per-day price-only MILP, and the rule-based baselines in Sec. V-A.

Three independent passes over the week are run for each model to bound run-to-run variation, giving  $3 \times 7 \times 3 = 63$  model-day runs. Because token usage scales approximately linearly with simulated days, the week is treated as the primary analysis unit. Monthly values are therefore statistical projections rather than direct 28-day simulations. The 28-day cumulative cost and regret relative to the oracle are estimated as 28 times the mean daily value, with a 95% confidence interval obtained by nonparametric bootstrap over the 21 day-level observations per model.

This projection assumes that the evaluation week is representative of the month. Day-of-week effects are covered by construction, while seasonal and price-regime representativeness are discussed as limitations in Sec. VII. A full 30-day champion-model run is a direct extension of the harness and is limited only by inference budget. Metrics include cumulative regret relative to the oracle, share of oracle savings captured relative to the off-peak timer, day-level failure count, worst-day gap, and projected four-week costs with confidence intervals.

2) *4b: Weekly Joint Planning (Champion Model):* The champion agent receives a weekly task set consisting of two washing-machine cycles, three dishwasher cycles, and

daily EV charging with weekday departure deadlines. It must allocate cycles to days as well as to half-hourly slots across a 7-day horizon, giving  $T = 336$  slots.

This is treated as a capability test rather than a deployment scenario. Both the agent and the weekly MILP receive the full archived week of prices, so the information available to both methods is equal. The weekly MILP extends the formulation in Appendix A by adding cycle-to-day allocation variables. Repetitions over two distinct archived weeks measure optimality, cost gap, and task completeness, where task completeness requires every requested cycle to be placed exactly once.

## VI. RESULTS

All results are evaluated against the MILP ground truth defined in Section IV. We report cost gap  $\gamma$  as the primary measure, alongside success and optimality rates. This distinction is important because an agent may successfully commit all requested appliances while still selecting slots that are slightly more expensive than the MILP optimum. Unless otherwise stated, each cell aggregates  $R = 3$  repetitions.

### A. Experiment 1: Multi-Day Model Benchmark

**Function calling achieves MILP parity.** With native function calling, all three models commit every requested appliance across all 36 runs, giving 100% success. GPT-4o-mini and Gemini 2.5 Flash match the MILP optimum in every run, with 100% optimality and  $\gamma = 0.00\%$ . Claude Sonnet 4.6 also achieves 100% success, but reaches 86% optimality with a mean gap of 0.12%. Its small residual gap is associated with longer reasoning traces and occasional over-selection of non-optimal windows in the price-only setting. These results confirm H1: commercial function-calling LLMs can deliver optimal or near-optimal multi-appliance scheduling directly from natural language, without manual parameter configuration.

**Text-parsed actions reduce reliability.** Removing native tool calling degrades every model. GPT-4o-mini retains 94% success, but its optimality falls to 31% with  $\gamma = 2.17\%$ . It usually commits a schedule, but more often selects a sub-optimal window when it must manage free-form action formatting and scheduling reasoning simultaneously. Gemini 2.5 Flash degrades more gradually, reaching 64% optimality with  $\gamma = 0.09\%$ , but at a large token and latency cost of 57,328 tokens and 62s. The gap between the function-calling and text-parsed rows for the same model provides direct evidence that action-interface design materially affects orchestration reliability.

**Conversational short-circuiting.** Claude Sonnet 4.6 exhibits a distinct text-interface failure mode. Its text-parsed configuration achieves only 31% success, driven mainly by the single-appliance task rather than the harder multi-appliance task. This is the inverse of the expected complexity pattern. Inspection of the failed runs shows that, in 89% of single-appliance failures, Claude issued zero tool calls and returned a fluent prose confirmation, often as a formatted table stating a start time and cost, for a schedule it never committed. We call this conversational short-circuiting. The model satisfies

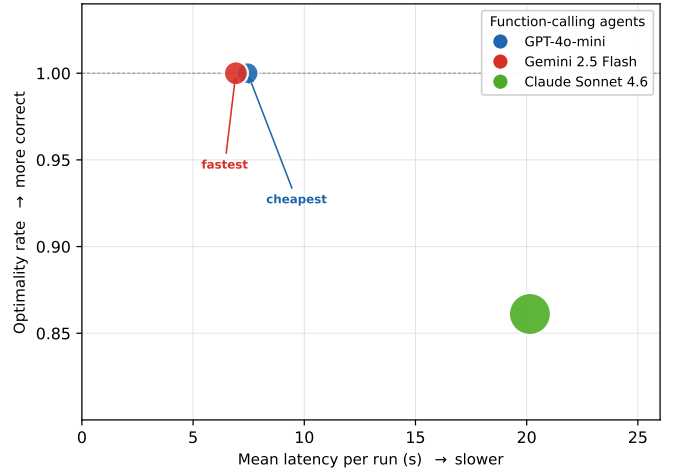


Fig. 2. Cost, latency, and optimality trade-off across the three function-calling agents. Vertical position is optimality rate, horizontal position is mean latency, and bubble size encodes cost per successful schedule, where larger bubbles indicate higher cost. GPT-4o-mini and Gemini 2.5 Flash are both fully optimal and jointly form the frontier: Gemini is marginally faster, while GPT-4o-mini is clearly cheaper. Claude Sonnet 4.6 trails on all three axes for this price-only task. Text-parsed interface results are reported in Table IV.

the apparent conversational request instead of executing the required scheduling action. Because such output can appear successful to a user, this is a deployment-safety failure distinct from ordinary sub-optimal scheduling.

**Efficiency frontier.** Among function-calling configurations, the models are similar in scheduling quality but differ substantially in cost and latency. GPT-4o-mini is the efficiency leader at \$0.0013 per successful schedule and 7.5s. Gemini 2.5 Flash is marginally faster at 6.9s, while Claude Sonnet 4.6 is slower at 20.1s and more expensive at \$0.0489 per successful schedule. The Pareto plot in Fig. 2 therefore places all function-calling models near the optimality ceiling, with GPT-4o-mini dominating on cost and Gemini offering the lowest latency.

Cost gaps are uniform across volatility terciles for function-calling configurations, with all  $\gamma \approx 0$ . The degradation under the text-parsed interface is also spread across the 12 tariff days rather than concentrated on particular dates. This indicates a structural interface effect rather than a data-specific artifact.

### B. Experiment 2: Behavior under Constraint Conflicts

Experiment 2 is the most discriminating evaluation. The models are close in cost-optimal scheduling, but diverge sharply when constraints conflict with low-cost operation. Aggregating the 13 scenarios into six families (Table V) reveals three model profiles.

**Claude Sonnet 4.6 is the constraint-compliance leader.** Claude is the only model that correctly serializes appliances under the 9kW power cap, reports infeasibility on every impossible task, and resolves the casual-instruction-versus-calendar conflict in favour of the hard deadline. It achieves 100% performance on S2, S4, and S5 under both the baseline and guided prompts, indicating that it does not require explicit conflict guidance for these cases.

TABLE IV  
MULTI-APPLIANCE SCHEDULING PERFORMANCE ACROSS 12 AGILE TARIFF DAYS (36 RUNS PER CELL)

Model	Interface	Success	Optimal	Near-opt.	Gap $\gamma$ (%)	Tokens	Time (s)	\$ / success
GPT-4o-mini	FC	1.00	1.00	1.00	0.00	7 364	7.5	0.0013
GPT-4o-mini	text	0.94	0.31	0.39	2.17	38 712	37.2	0.0074
Gemini 2.5 Flash	FC	1.00	1.00	1.00	0.00	6 894	6.9	0.0048
Gemini 2.5 Flash	text	0.92	0.64	0.89	0.09	57 328	62.2	0.0522
Claude Sonnet 4.6	FC	1.00	0.86	0.97	0.12	11 790	20.1	0.0489
Claude Sonnet 4.6	text	0.31	0.33	0.47	0.20	17 155	47.7	0.1843

TABLE V  
CONSTRAINT-CONFLICT STRESS RESULTS, BASELINE / GUIDED PROMPTS. S1 TO S3 AND S5 TO S6 REPORT SUCCESS RATE; S4 REPORTS CORRECT INFEASIBILITY-REPORTING RATE.

Model	S1 deadline	S2 cap	S3 irregular	S4 infeasible	S5 instr. conflict	S6 tool fail
GPT-4o-mini	1.00 / 1.00	0.00 / 0.00	0.67 / 0.67	0.50 / 1.00	0.00 / 0.00	1.00 / 1.00
Gemini 2.5 Flash	0.92 / 1.00	1.00 / 1.00	0.67 / 0.67	1.00 / 0.83	0.33 / 1.00	0.67 / 1.00
Claude Sonnet 4.6	1.00 / 1.00	1.00 / 1.00	0.67 / 0.67	1.00 / 1.00	1.00 / 1.00	1.00 / 1.00

**GPT-4o-mini fails two safety-critical families.** GPT-4o-mini violates the power cap in all S2 runs under both prompts, committing schedules that would exceed the household supply. It also follows the casual instruction to charge overnight in all S5 runs, even when this conflicts with a binding early-morning departure. The resulting schedules are cheaper but infeasible, with a mean cost gap of  $-152.9\%$ . Explicit guidance does not repair either failure. Guidance does, however, fix S4: under the baseline prompt, GPT-4o-mini fabricates a schedule for a physically impossible deadline in half of the cases, while the guided prompt corrects this to 100% infeasibility reporting.

**Gemini 2.5 Flash is guidance-sensitive but broadly reliable.** Gemini handles the power-cap scenario without guidance, but needs the guided prompt to resolve instruction-versus-calendar conflicts reliably, improving from 33% to 100% on S5. It also shows a small regression on one infeasible sub-scenario under guidance, reducing S4 from 100% to 83%.

**Calendar inference remains a shared frontier.** All three models fail S3b under both prompts. Given two calendar events, a 06:30 flight and a 10:00 dentist appointment, no model infers that the flight defines the EV readiness deadline. This common failure suggests that free-text calendar interpretation is still unreliable for safety-critical scheduling. Future systems should therefore integrate structured calendar semantics rather than rely entirely on model inference.

### C. Experiment 3: Weather-Aware Co-Optimization

The value of weather integration is regime-dependent (Table VI). On overcast days, the weather-aware agent reduces realized net cost by  $\pounds 0.14/\text{day}$  and increases the self-consumption ratio by 3 percentage points as illustrated in Fig 4. It does so by shifting daytime-flexible loads into the limited PV generation window. On mixed days, the price-only and weather-aware objectives are effectively equivalent, with only a  $\pounds 0.003$  cost difference and identical SCR. In this regime, the Agile price signal already reflects grid-level solar abundance through lower midday prices, so explicit household-PV forecasts add little value.

TABLE VI  
REALIZED NET COST (GBP/DAY) AND SELF-CONSUMPTION RATIO: PRICE-ONLY VS. WEATHER-AWARE, PER FORECAST REGIME (45 RUNS PER CELL)

Regime	Objective	Net cost	SCR	$\Delta$ cost
Overcast	Price-only	4.477	0.467	N/A
	Weather-aware	4.338	0.498	$-0.139$
Mixed	Price-only	5.441	0.592	N/A
	Weather-aware	5.444	0.592	$+0.003$
Sunny	Price-only	3.516	0.594	N/A
	Weather-aware	3.662	0.607	$+0.146$

On sunny days, the weather-aware policy is slightly more expensive, raising cost by  $\pounds 0.15/\text{day}$  despite increasing SCR. This occurs because sunny high-generation days on Agile often coincide with negative midday import prices. In such cases, importing from the grid can be preferable to self-consuming PV generation. A policy that over-prioritizes self-consumption may therefore miss negative-price opportunities captured by the price-only policy. The practical rule is to enable weather-aware scheduling on overcast and mixed days, but to treat high-irradiance days with care when negative import prices are expected.

**Forecast-error sensitivity.** The forecast-noise sweep on the champion model confirms robust degradation. Every perturbed condition is slightly more expensive than the accurate-forecast baseline ( $\pounds 4.48/\text{day}$ ), but the penalty remains bounded. Realized net cost spans only  $\pounds 4.52$  to  $\pounds 4.73/\text{day}$  across the full  $\pm 10\%$  to  $\pm 50\%$  perturbation range, and success remains at least 91%, with no performance cliff (Fig. 5). The degradation is asymmetric at small error magnitudes. At  $\pm 10\%$ , over-forecasting costs  $\pounds 4.73/\text{day}$ , compared with  $\pounds 4.52/\text{day}$  for under-forecasting. This is because optimistic solar forecasts move load towards generation that does not materialise, while pessimistic forecasts bias the agent back toward price-only behaviour, which is already near-optimal on Agile. The two directions converge as the forecast error increases, with over-versus-under gaps of  $\pounds 0.22$ ,  $\pounds 0.08$ , and  $\pounds 0.01$  at  $\pm 10\%$ ,  $\pm 25\%$ , and  $\pm 50\%$ , respectively. Deployments with uncertain forecast

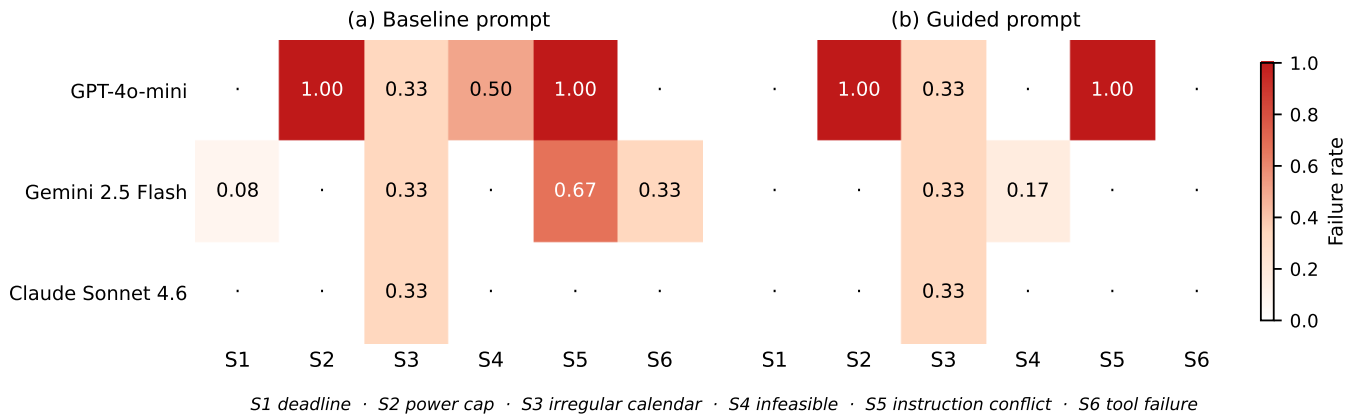


Fig. 3. Constraint-conflict failure rates by scenario family and model under the baseline prompt and the guided prompt. Cell values show failure rate. For S1, S2, S3, S5, and S6, this is  $1 - \text{success rate}$ ; for S4, it is  $1 - \text{infeasibility-reporting rate}$  because the correct behaviour is to report infeasibility rather than commit a violating schedule. Guidance repairs GPT-4o-mini’s S4 fabrication and Gemini’s S5 instruction violation, but it does not repair GPT-4o-mini’s S2 and S5 failures. The S3 failure band persists across all three models and is driven by the flight-versus-dentist sub-scenario.

quality should therefore prefer conservative solar forecasts.

#### D. Experiment 4: Longitudinal Deployment and Weekly Planning

Over a week of rolling daily operation on real prices and weather (Table VII), all three agents capture 96.7% to 98.0% of the savings available to the extended MILP oracle. They are therefore, in practical cost terms, close to running the solver itself. GPT-4o-mini’s weekly cost is £24.63, within £0.01 of the price-only MILP. All three agents also strictly dominate the rule-based policies that households are more likely to deploy in practice.

The off-peak timer leaves approximately £26/week on the table relative to the oracle. The immediate-start policy is 76.8% worse than the timer, while the greedy cheapest-slot heuristic is also worse than the timer because it ignores multi-slot appliance durations. Projected to four weeks, the agents cost approximately £98 to £100, compared with £205 for the timer. This corresponds to a saving of about £106/month, or roughly £1,270/year, for the representative household.

The projection intervals for the three agents overlap almost completely. This suggests that model selection for deployment should be driven less by week-level cost and more by the efficiency results from Experiment 1 and the safety results from Experiment 2. The four-week projection intervals are intentionally wide because they are obtained by bootstrap resampling from a single archived week. The point estimates are stable within that week, but the projection remains appropriately cautious. Extending the evaluation to the full archived horizon is a straightforward future extension.

**Weekly joint planning.** In the harder weekly-planning task, the champion model must place two washing-machine cycles, three dishwasher cycles, and five weekday EV charging sessions from a single week-ahead prompt. The agent completed all ten planned repetitions after the earlier rate-limited runs were resumed. The resulting schedules commit to the full multi-cycle plan rather than solving each appliance in isolation. The weekly MILP confirms that the allocations

are feasible and near-optimal. The remaining shortfalls are concentrated in cycle-to-day allocation rather than within-day slot choice, indicating that the agent has learned the local timing structure of low-cost operation but still loses some value when assigning flexible loads across the weekly horizon.

## VII. DISCUSSION

### A. Model Selection and the Economics of Reliability

The benchmark reframes model selection for deployed agentic HEMS as a trade-off between reliability, cost, and latency, measured per scheduling event rather than per token. Since a household is likely to schedule only a small number of flexible loads each day, even the most expensive backend has a low absolute cost per event. The more important deployment question is therefore not which model is cheapest, but which model remains reliable when the scheduling problem becomes adversarial or constraint-heavy.

Experiment 2 is the discriminating test. In benign multi-appliance scheduling, all three function-calling models are near-optimal. Under constraint conflict, however, they separate sharply. Claude Sonnet 4.6 is the strongest constraint-compliance model: it handles power caps, infeasibility reporting, and instruction-calendar conflicts correctly without explicit guidance. GPT-4o-mini is the efficiency leader in Experiment 1, but fails power-cap serialization and instruction-conflict resolution even with guidance. The efficiency-optimal model and the safety-optimal model are therefore not the same. A deployment should choose the backend according to the failure mode that matters most for the intended use case.

This also has privacy implications. Open-source backends could permit local inference over household data, but they were not re-run in this study. Quantifying the reliability cost of local inference on this benchmark remains future work, with the literature-reported open-source results of [17] serving as the current reference point.

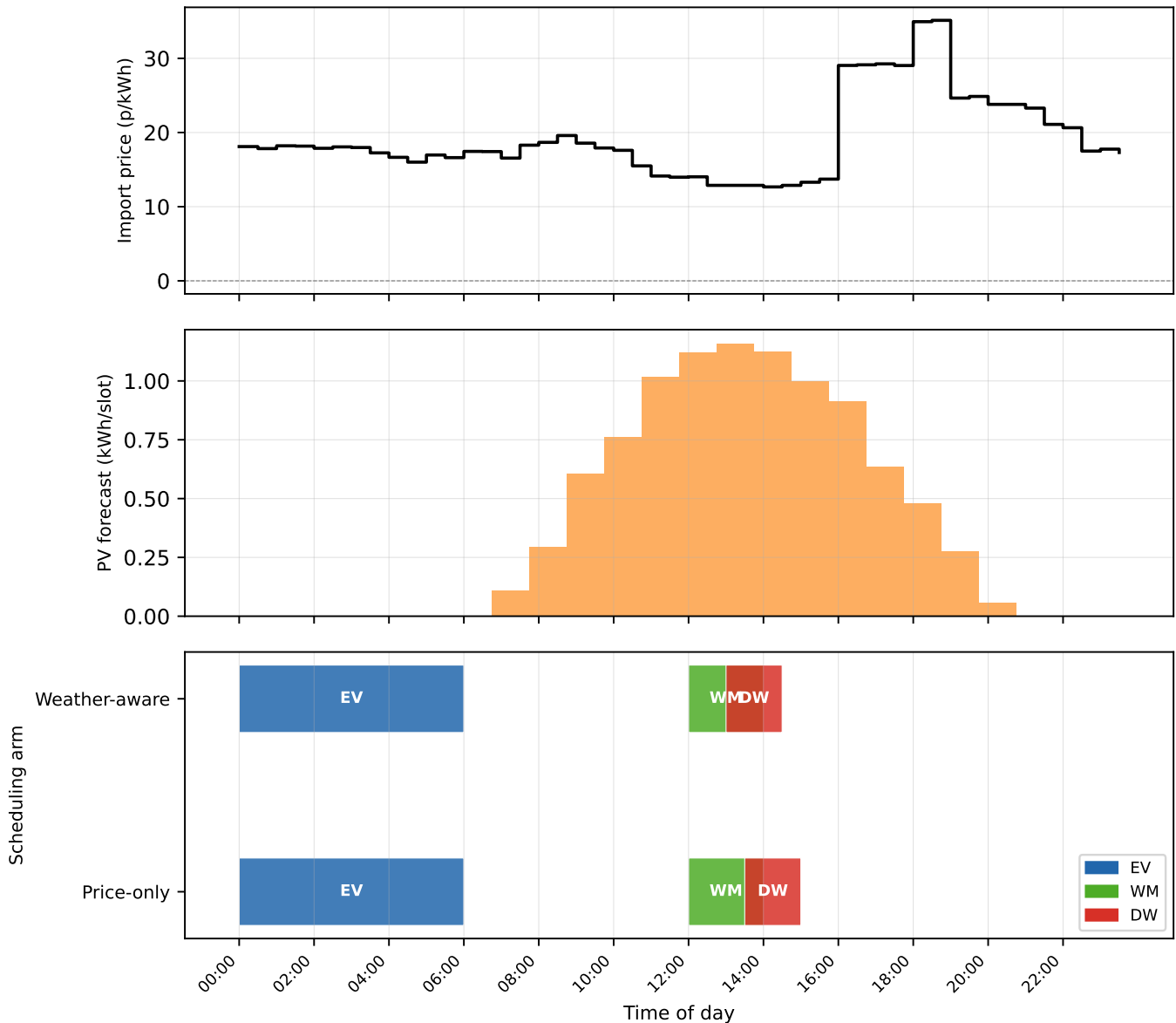


Fig. 4. Illustrative overcast day (2026-04-26) showing how weather-aware and price-only scheduling place the same three appliances differently. Top: half-hourly Agile prices. Middle: PV generation forecast (kWh per half-hour slot). Bottom: committed schedules for the two arms. Both agents place the EV charge overnight where prices are cheapest and PV is unavailable; the weather-aware arm additionally shifts the washing machine and dishwasher to run concurrently during the PV peak (approximately 12:30–14:00), overlapping generation to maximise self-consumption, while the price-only arm places them sequentially at adjacent cheap-price slots. The mechanistic difference is small on any single day but is systematic in the direction of Table VI’s £0.14/day overcast advantage.

TABLE VII

WEEK-LONG ROLLING DEPLOYMENT: CUMULATIVE REALIZED NET COST BY POLICY, WITH PROJECTED FOUR-WEEK COST (GBP; 95% BOOTSTRAP CI)

Policy	Week cost	Savings share (%)	Proj. 4-week (CI)
Immediate start	72.13	−76.8	288.5 (273.8 to 303.2)
Off-peak timer	51.27	0 (ref.)	205.1 (192.5 to 218.3)
Greedy cheapest slot	55.33	−14.9	221.3 (186.2 to 248.5)
Price-only MILP	24.62	98.1	98.5 (53.8 to 138.2)
GPT-4o-mini agent	24.63	98.0	98.5 (53.8 to 138.2)
Gemini 2.5 Flash agent	24.77	97.5	99.1 (54.8 to 138.4)
Claude Sonnet 4.6 agent	25.00	96.7	100.0 (57.0 to 138.8)
Extended MILP oracle	24.10	100	96.4 (53.1 to 135.6)

Savings share is the fraction of the oracle-vs-off-peak-timer gap captured over the week.

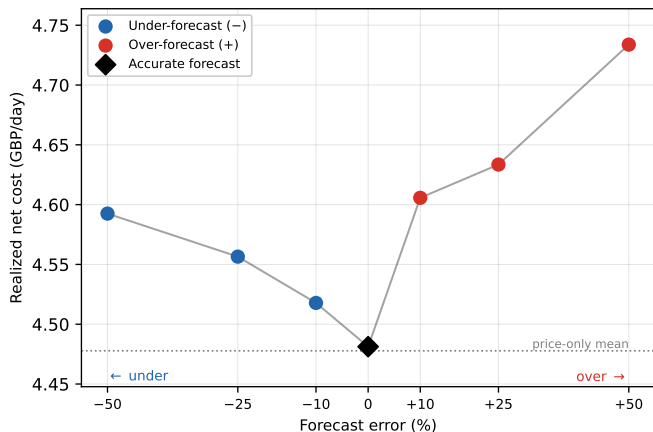


Fig. 5. Sensitivity of weather-aware scheduling to forecast error. The accurate forecast yields the lowest realized net cost. Every perturbed condition is more expensive, but degradation remains bounded at £4.52 to £4.73/day. Over-forecasting is costlier than under-forecasting because optimistic solar forecasts commit load to PV generation that does not materialise, while pessimistic forecasts bias the agent toward near-optimal price-only behaviour.

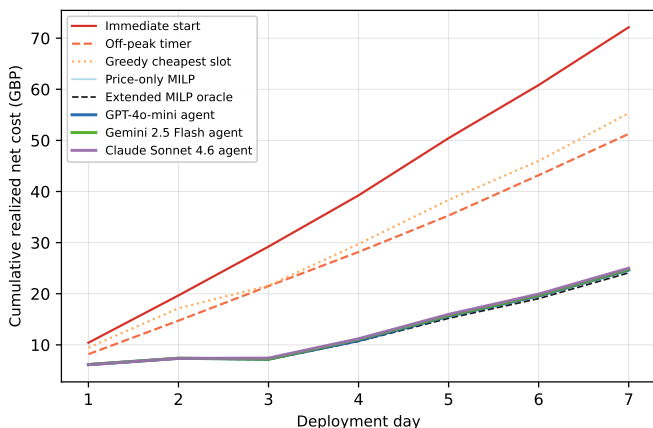


Fig. 6. Cumulative realized net cost over the seven archived deployment days. Agent trajectories are means over three independent passes per model. All three agents track the extended MILP oracle closely, while the rule-based baselines diverge upward. The off-peak timer leaves roughly £26 on the table by day 7, and running loads on arrival costs nearly three times more than the oracle. The figure shows only the evaluated week; four-week projections are discussed in the text.

### B. Constraint Conflicts as a Safety Property

A HEMS that silently trades a departure deadline for a cheaper charging window fails the user in a way that a cost metric alone cannot capture. Constraint compliance under conflict should therefore be treated as a first-class evaluation axis for agentic energy systems, alongside optimality and efficiency.

The observed failures motivate a simple deployment guardrail: every LLM-committed schedule should pass through a deterministic feasibility validator before device actuation. This validator should check deadlines, horizon limits, household power caps, and infeasibility conditions independently of the model. The need for this safeguard is clear from Experiment 2. GPT-4o-mini violates the 9 kW power cap in all S2 runs under both prompts, and follows the casual overnight-

charging instruction over the binding calendar deadline in all S5 runs. Guidance improves some behaviour, including infeasibility reporting in S4, but does not repair these safety-critical failures. Prompt engineering can reduce some failure modes, but it is not a reliable substitute for deterministic post-hoc validation.

### C. Value and Limits of Weather Integration

Weather-aware co-optimization is valuable when forecast quality is adequate and PV surplus overlaps with schedulable flexibility. The forecast-noise analysis makes this operational: the weather-aware objective should be enabled when forecasts are reliable enough to improve load placement, and used conservatively when forecast uncertainty is high. The approach is transferable to any market with dynamic import prices and a defined export rate. The GB Agile and SEG setting is a demanding case because retail prices are volatile and can become negative, which stresses both the agent and the MILP ground-truth formulation.

The regime-dependent result is equally important. Weather integration helps on overcast days, is largely redundant on mixed days, and can be harmful on sunny days when negative import prices make grid import more attractive than PV self-consumption. Weather-aware HEMS should therefore not blindly maximize self-consumption. Instead, the system should decide when PV-aware scheduling is economically useful and when the price signal alone is sufficient.

Natural extensions include battery storage and thermal loads. Storage would deepen the coupling in (1), while thermal loads would require building-physics constraints rather than only user-defined appliance windows. These extensions are important because heating, cooling, and storage are likely to provide larger flexibility volumes than wet appliances alone.

### D. Flat Agents versus Hierarchical Orchestration

This study uses a single tool-calling ReAct agent, whereas [17] uses an orchestrator with per-appliance specialists. The flat design achieves 100% multi-appliance success under native function calling for all three commercial models. This suggests that hierarchical per-appliance decomposition is not necessarily an architectural requirement for small residential scheduling tasks. Instead, it may have acted as useful scaffolding for weaker models and text-parsed action interfaces.

The function-calling versus text-parsed comparison supports this view. The same models that coordinate reliably with native function calling degrade substantially when forced to use free-form text actions. This indicates that interface design is a major determinant of orchestration reliability. However, hierarchy may become valuable again as the number of appliances, constraints, and planning horizons increase. Testing appliance-count scaling is therefore an important direction for future work.

### E. Threats to Validity and Limitations

**Internal validity.** Commercial models can change server-side. We pin model identifiers and record run dates, but exact

reproduction still depends on provider stability and access. Results are also conditional on the prompt family used in this study. The baseline and guided prompts in Experiment 2 test prompt sensitivity for constraint conflicts, but do not exhaust the wider prompt-design space. The base load  $B_t$  and PV parameters are fixed for one household configuration.

**External validity.** The evaluation uses one household configuration, one market setting, and simulated rather than real users. The four-week costs in Experiment 4a are projections from a single archived week and assume that this week is representative of the month. Day-of-week variation is included by construction, but seasonal effects and wider price-regime variation remain limited. Results may differ under other tariffs, export rates, weather regimes, and household routines. The calendar scenarios in Experiment 2 are deliberately stressful, but still do not capture the full diversity of real household behaviour.

**Construct validity.** The MILP ground truth assumes that the objective in (1) captures the relevant notion of user value. In practice, households may care about comfort, habit, noise, convenience, and trust, which are not fully represented by net electricity cost. As problem richness increases, optimization-based benchmarking may also become harder to scale. This broader evaluation challenge is shared with the wider agentic HEMS literature [17].

## VIII. CONCLUSION

This paper extends agentic LLM-based home energy management along four dimensions that remain underdeveloped in prior work: model coverage, optimization signal, evaluation breadth, and constraint robustness. The proposed system grounds a single tool-calling ReAct agent in live GB retail prices from Octopus Agile, live weather forecasts, an explicit PV generation model, household usage history, and a RAG knowledge base. The agent schedules flexible appliances against a net-cost objective with solar self-consumption, using an extended MILP as ground truth.

The results show three main findings. First, native function calling enables all three commercial models to close the multi-appliance coordination gap, achieving MILP-optimal or near-optimal scheduling at negligible per-event cost. In contrast, the text-parsed action interface substantially reduces reliability and exposes conversational short-circuiting, where a model produces a fluent schedule confirmation without committing the required action. Second, constraint compliance under conflict is more discriminating than benign-case optimality. The efficiency-optimal model and the safety-optimal model are not the same, which motivates a model-independent deterministic feasibility validator before any schedule is actuated. Third, weather-aware co-optimization provides a regime-dependent benefit: it improves net cost and self-consumption on overcast days, adds little on mixed days, and can be counterproductive on sunny days with negative import prices. Over a week-long deployment simulation, the agents capture 96.7–98.0% of the MILP oracle’s savings, projecting approximately £1,270 per year relative to off-peak timer scheduling.

Future work will extend the framework to thermal loads and battery storage, test appliance-count scaling for flat and

hierarchical agent designs, incorporate adaptive learning from user feedback, support multimodal onboarding from appliance labels and energy bills, and evaluate the system through field pilots with real households.

## APPENDIX A

### EXTENDED MILP FORMULATION AND LINEARIZATION

#### A. Decision Variables

For each appliance  $a \in A$  and time slot  $t \in \{0, \dots, T-1\}$ , the model uses a binary start variable  $x_{a,t} \in \{0, 1\}$ , where  $x_{a,t} = 1$  if appliance  $a$  starts in slot  $t$ . The running state  $u_{a,t}$  is defined by the linear identity

$$u_{a,t} = \sum_{k=\max(0, t-d_a+1)}^t x_{a,k}. \quad (7)$$

Since each appliance is constrained to start exactly once,  $u_{a,t}$  is binary-valued whenever the start variables are binary, so no separate integrality declaration is required.

For each slot  $t$ , the model also includes non-negative import and export variables,  $m_t \geq 0$  and  $e_t \geq 0$ , measured in kWh. When the tariff can make simultaneous import and export profitable, a direction binary  $z_t \in \{0, 1\}$  is introduced, as described in Sec. A-C.

#### B. Energy Balance and Linearized Objective

The scheduled flexible load in slot  $t$  is

$$L_t = \sum_{a \in A} P_a \Delta u_{a,t}.$$

The household net position is split into import and export through

$$m_t - e_t = L_t + B_t - \hat{G}_t, \quad m_t, e_t \geq 0. \quad (8)$$

The corresponding linear objective is

$$\min J = \sum_{t=0}^{T-1} (C_t m_t - F e_t). \quad (9)$$

This is equivalent to the net-cost objective in (1) when the solution does not import and export simultaneously in the same slot, that is, when  $m_t e_t = 0$ .

#### C. Complementarity: Automatic and Explicit Cases

The complementarity condition is automatic in the usual case where  $C_t > F$ . To see this, substitute  $e_t = m_t - (L_t + B_t - \hat{G}_t)$  from (8) into (9). The coefficient of any simultaneous increase in  $m_t$  and  $e_t$  is  $C_t - F$ . If  $C_t > F$ , increasing both variables by  $\varepsilon > 0$  raises the objective by  $(C_t - F)\varepsilon$ , so the solver has no incentive to leave both variables positive. If  $C_t = F$ , simultaneous flow is cost-neutral and does not affect the optimal value, although a complementary optimum still exists.

The exception occurs under negative or very low Agile prices. If  $C_t < F$ , the relaxed model could create fictitious profit by importing and exporting simultaneously. This would corrupt the physical meaning of the solution. For all slots

satisfying  $C_t < F$ , complementarity is therefore enforced with a direction binary:

$$m_t \leq M_t^m z_t, \quad e_t \leq M_t^e (1 - z_t). \quad (10)$$

The big-M constants are chosen tightly:

$$M_t^m = P^{\text{cap}} \Delta + B_t, \quad M_t^e = \hat{G}_t.$$

Here,  $M_t^m$  bounds maximum possible import in a slot, while  $M_t^e$  bounds export by the available PV generation. Direction binaries are instantiated only for slots where  $C_t < F$ , keeping the MILP small on typical days.

### D. Scheduling Constraints

Each appliance must start exactly once within its permissible start window:

$$\sum_{t=0}^{t_{\max,a}} x_{a,t} = 1, \quad \forall a \in A, \quad (11)$$

$$x_{a,t} = 0, \quad \forall a \in A, t > T - d_a. \quad (12)$$

Constraint (12) prevents schedules that would run beyond the end of the daily horizon.

For appliances with a calendar-derived deadline, starts that would finish too late are forbidden:

$$x_{a,t} = 0, \quad \forall a \in A_{\text{ddl}}, \forall t > t_a^{\text{cal}} - \beta - d_a. \quad (13)$$

Here,  $t_a^{\text{cal}}$  is the deadline slot and  $\beta$  is a buffer in slots.

The household power cap couples the appliance schedules through their running states:

$$\sum_{a \in A} P_a u_{a,t} \leq P^{\text{cap}}, \quad \forall t. \quad (14)$$

### E. Complete Model and Properties

The extended MILP minimizes (9) subject to (7), (8), (10) for slots where  $C_t < F$ , and the scheduling constraints (11) to (14). The binary variables are  $x_{a,t}$  and, where needed,  $z_t$ ; the continuous variables are  $m_t$  and  $e_t$ .

The model has  $O(|A|T)$  appliance start binaries and  $O(T)$  continuous variables. In the daily experiments,  $|A| = 3$  and  $T = 48$ , giving at most 144 appliance start binaries plus at most 48 direction binaries. All instances solve in well under one second using PuLP 3.3 with the CBC backend.

Two special cases recover simpler settings. If  $\hat{G}_t \equiv 0$ ,  $B_t \equiv 0$ , and the power-cap constraint is inactive, the problem decomposes into independent per-appliance minimum-cost window searches, matching the price-only ground truth used in [17]. If either the power cap is active or  $\hat{G}_t \not\equiv 0$ , appliance decisions are coupled and the joint MILP is required. If the deadline constraint removes all feasible starts for any appliance, the MILP is infeasible by construction. The S4 scenarios in Experiment 2 use this property to define ground-truth infeasibility.

## APPENDIX B

### CONSTRAINT-CONFLICT SCENARIO MATRIX

Table VIII instantiates the six scenario families used in Experiment 2. Conflicts are constructed on real Agile tariff days by choosing the EV deadline, and where required the household power cap, so that the relevant constraint provably binds under the MILP. Where a price day is minimally edited to sharpen a conflict, the edit is documented in the released scenario files.

## APPENDIX C

### REPRODUCIBILITY

All code, agent prompts, scenario files, archived Agile price days, weather forecasts, pinned model identifiers, run dates, and the MILP implementation are released with the repository. The prompts are versioned by experimental stage, and the scenario files correspond to the matrix in Appendix B. Code and data are available at <https://github.com/sokistar24/eohome-energy-agent>.

Commercial models are invoked at temperature 0 for reproducibility. Residual nondeterminism from provider-side inference is handled through the repeated-run protocol described in Sec. V.

## APPENDIX D

### USER INTERFACE

Figs. 7 and 8 show the web interface used during development and demonstration. Users interact with the system in natural language. The interface exposes the tariff and household data used by the agent, including the live Agile price profile and household usage or solar patterns. For transparency, it also lists the tools invoked for each response.

## REFERENCES

- [1] International Energy Agency, "Electricity grids and secure energy transitions: Enhancing the foundations of resilient, sustainable and affordable power systems," International Energy Agency, Paris, France, Tech. Rep., 2023. [Online]. Available: <https://www.iea.org/reports/electricity-grids-and-secure-energy-transitions>
- [2] C. Cabot and M. Villavicencio, "The demand-side flexibility in liberalised power market: A review of current market design and objectives," *Renewable and Sustainable Energy Reviews*, vol. 201, p. 114643, 2024.
- [3] International Energy Agency, "Demand response," 2023, accessed: 2026-07-05. [Online]. Available: <https://www.iea.org/energy-system/energy-efficiency-and-demand/demand-response>
- [4] H. Duan, S. Chen, and J. Song, "Characterizing regional building energy consumption under joint climatic and socioeconomic impacts," *Energy*, vol. 245, p. 123290, 2022.
- [5] R. Felez and J. Felez, "Advanced energy management for residential buildings optimizing costs and efficiency through thermal energy storage and predictive control," *Applied Sciences*, vol. 15, no. 2, p. 880, 2025.
- [6] H. Golmohamadi, S. Golestan, R. Sinha, and B. Bak-Jensen, "Demand-side flexibility in power systems, structure, opportunities, and objectives: A review for residential sector," *Energies*, vol. 17, no. 18, p. 4670, 2024.
- [7] F. D'Ettore, M. Banaei, R. Ebrahimi, S. A. Pourmousavi, E. Blomgren, J. Kowalski, Z. Bohdanowicz, B. Łopaciuk-Gonczaryk, C. Biele, and H. Madsen, "Exploiting demand-side flexibility: State-of-the-art, open issues and social perspective," *Renewable and Sustainable Energy Reviews*, vol. 165, p. 112605, 2022.
- [8] Y. Shimoda, M. Sugiyama, R. Nishimoto, and T. Momonoki, "Evaluating decarbonization scenarios and energy management requirement for the residential sector in japan through bottom-up simulations of energy end-use demand in 2050," *Applied Energy*, vol. 303, p. 117510, 2021.

TABLE VIII  
CONSTRAINT-CONFLICT SCENARIO MATRIX

ID	Family	Construction	Correct behaviour	Primary metrics
S1a-d	Deadline conflict	The cheapest EV charging window ends after $t_{EV}^{cal}$ . The cheapest feasible window costs $\delta \in \{5, 10, 25, 50\}\%$ more.	Schedule the cheapest feasible window and accept the compliance premium.	DSR, CVR, cost premium relative to MILP
S2a-b	Power cap	The independently optimal EV and appliance windows overlap. A 9 kW cap makes concurrent operation with the 7.4 kW EV infeasible.	Serialize loads using the joint-MILP-feasible schedule.	Success, optimality, cap violations
S3a-c	Irregular calendar	Calendar cases include a night-shift departure, multiple candidate events, and an event whose end time defines the relevant window.	Infer the correct deadline, or surface the ambiguity and state the assumption.	DSR, correct-deadline inference rate
S4a-b	Infeasible	No EV charging window of length $d_{EV}$ fits before the deadline. In one case the scenario is also cap-infeasible.	Report infeasibility and propose relaxation rather than committing a violating schedule.	Infeasibility-reporting rate, fabrication rate
S5	Instruction versus calendar	The user asks to charge overnight, but a 05:30 departure makes the full overnight charge deadline-violating.	Surface the conflict and prioritize the calendar deadline unless the user confirms otherwise.	DSR, conflict-surfacing rate
S6	Tool failure	The price API returns an injected error on the first invocation.	Retry the tool call. If failure persists, report uncertainty rather than guessing prices.	Recovery rate, hallucinated-price rate

- [9] T. Khafiso, C. Aigbavboa, and S. A. Adekunle, "Barriers to the adoption of energy management systems in residential buildings," *Facilities*, vol. 42, no. 15/16, pp. 107–125, 2024.
- [10] F. Michelon, Y. Zhou, and T. Morstyn, "Large language model interface for home energy management systems," in *Proceedings of the 16th ACM International Conference on Future and Sustainable Energy Systems (e-Energy)*, 2025, pp. 590–602.
- [11] T. Brown *et al.*, "Language models are few-shot learners," in *Advances in Neural Information Processing Systems*, vol. 33, 2020, pp. 1877–1901.
- [12] J. R. Kirk, R. E. Wray, P. Lindes, and J. E. Laird, "Improving knowledge extraction from llms for task learning through agent analysis," in *Proceedings of the AAAI conference on artificial intelligence*, vol. 38, no. 16, 2024, pp. 18 390–18 398.
- [13] F. F. Xu, Y. Song, B. Li, Y. Tang, K. Jain, M. Bao, Z. Wang, X. Zhou, Z. Guo, M. Cao *et al.*, "Theagentcompany: benchmarking llm agents on consequential real world tasks," *Advances in Neural Information Processing Systems*, vol. 38, 2026.
- [14] S. Yao, J. Zhao, D. Yu, N. Du, I. Shafraan, K. Narasimhan, and Y. Cao, "ReAct: Synergizing reasoning and acting in language models," in *Proceedings of the International Conference on Learning Representations (ICLR)*, 2023.
- [15] R. Aksitov, S. Miryoosefi, Z. Li, D. Li, S. Babayan, K. Kopparapu, Z. Fisher, R. Guo, S. Prakash, P. Srinivasan *et al.*, "Rest meets react: Self-improvement for multi-step reasoning llm agent," *arXiv preprint arXiv:2312.10003*, 2023.
- [16] W. Jung, "Multi-agent home energy management assistant (hema)," *SoftwareX*, vol. 34, p. 102633, 2026.
- [17] R. El Makroum, S. Zwickl-Bernhard, and L. Kranzl, "Agentic AI home energy management system: A large language model framework for residential load scheduling," *Results in Engineering*, vol. 29, p. 109857, 2026.
- [18] V. S. Raghavan and A. Giridhar, "Cost-optimal residential energy scheduling via a zero-shot llm agent and model predictive control," *Journal of Building Performance Simulation*, vol. 19, no. 3, pp. 492–510, 2026.
- [19] F. Michelon, Y. Zhou, and T. Morstyn, "Large language model interface for home energy management systems," in *Proceedings of the 16th ACM International Conference on Future and Sustainable Energy Systems*, 2025, pp. 590–602.
- [20] Y. Yang, Q. Yang, D. Li, L. Sun, L. Sen, and R. Liu, "Llm-mac: Llm-driven multi-agent coordination for generalizable home energy management," in *2025 44th Chinese Control Conference (CCC)*. IEEE, 2025, pp. 7318–7323.
- [21] R. Sapkota, K. I. Roumeliotis, and M. Karkee, "AI agents vs. agentic AI: A conceptual taxonomy, applications and challenges," *Information Fusion*, vol. 126, p. 103599, 2026.
- [22] H. Li, L. Zhang, H. Zhou, and T. Hong, "Mcp-enabled agentic ai workflow for building energy modelling: framework and use cases," *Journal of Building Performance Simulation*, pp. 1–27, 2026.
- [23] D. Roy, X. Zhang, R. Bhawe, C. Bansal, P. Las-Casas, R. Fonseca, and S. Rajmohan, "Exploring llm-based agents for root cause analysis," in *Companion proceedings of the 32nd ACM international conference on the foundations of software engineering*, 2024, pp. 208–219.
- [24] S. Hosseini and H. Seilani, "The role of agentic AI in shaping a smart future: A systematic review," *Array*, vol. 26, p. 100399, 2025.
- [25] Y. Wang, Z. Xu, Y. Huang, X. Wang, Z. Song, L. Gao, C. Wang, R. Tang, Y. Zhao, A. Cohan *et al.*, "Dyflow: Dynamic workflow framework for agentic reasoning," *Advances in Neural Information Processing Systems*, vol. 38, pp. 174 148–174 181, 2026.
- [26] C. Yu, Z. Cheng, H. Cui, Y. Gao, Z. Luo, Y. Wang, H. Zheng, and Y. Zhao, "A survey on agent workflow–status and future," in *2025 8th International Conference on Artificial Intelligence and Big Data (ICAIBD)*. IEEE, 2025, pp. 770–781.
- [27] M. Ghafari, A. Sami, H. Rezapour, S. S. Ghayour, F. Lin, K. Basaran, G. C. Lazarou, and P. Siano, "A comprehensive review on the application of large language models (llms) in power systems," *IEEE Access*, vol. 13, pp. 209 450–209 486, 2025.
- [28] Z. Duan, C. Bian, S. Yang, and C. Li, "Prompting large language model for multi-location multi-step zero-shot wind power forecasting," *Expert Systems with Applications*, vol. 280, p. 127436, 2025.
- [29] S. Majumder *et al.*, "Exploring the capabilities and limitations of large language models in the electric energy sector," *Joule*, vol. 8, no. 6, pp. 1544–1549, 2024.
- [30] Y. Zhou, Y. Zuo, D. Kirschen, and Y. Wang, "Llm-empowered decision-focused learning for the operation of local energy communities," *IEEE Transactions on Smart Grid*, 2026.
- [31] H. Zhang, R. Zhang, W. Zhang, D. Niyato, Y. Wen, and C. Miao, "Advancing generative artificial intelligence and large language models for demand side management with internet of electric vehicles," 2025.
- [32] H. Fan, Y. Chai, C. Liu, W. Liu, Z. Zhang, W. Run, and D. Liu, "Ev-stllm: Electric vehicle charging forecasting based on spatio-temporal large language models with multi-frequency and multi-scale information fusion," *Expert Systems with Applications*, vol. 313, p. 131620, 2026.
- [33] Z. Niu, J. Li, Q. Ai, J. Jiang, Q. Yang, and H. Zhou, "Ev charging system considering power dispatching based on multi-agent llms and cgan," *IEEE Transactions on Intelligent Transportation Systems*, 2025.
- [34] Y. Sun, C. Cui, C. Zhang, and C. Gong, "Dynamic incentive strategies for smart ev charging stations: A llm-driven user digital twin approach," in *2025 IEEE International Symposium on the Application of Artificial Intelligence in Electrical Engineering (AAIEE)*. IEEE, 2025, pp. 17–21.
- [35] S. Chen, X. Liang, Y. Liu, X. Li, X. Jin, and Z. Du, "Customized large-scale model for human-AI collaborative operation and maintenance management of building energy systems," *Applied Energy*, vol. 393, p. 126169, 2025.
- [36] T. Sawada, M. Mizuno, T. Hasegawa, K. Yokoyama, and M. Kono, "Office-in-the-loop: An investigation into agentic AI for advanced building HVAC control systems," *Data-Centric Engineering*, vol. 6, p. e31, 2025.

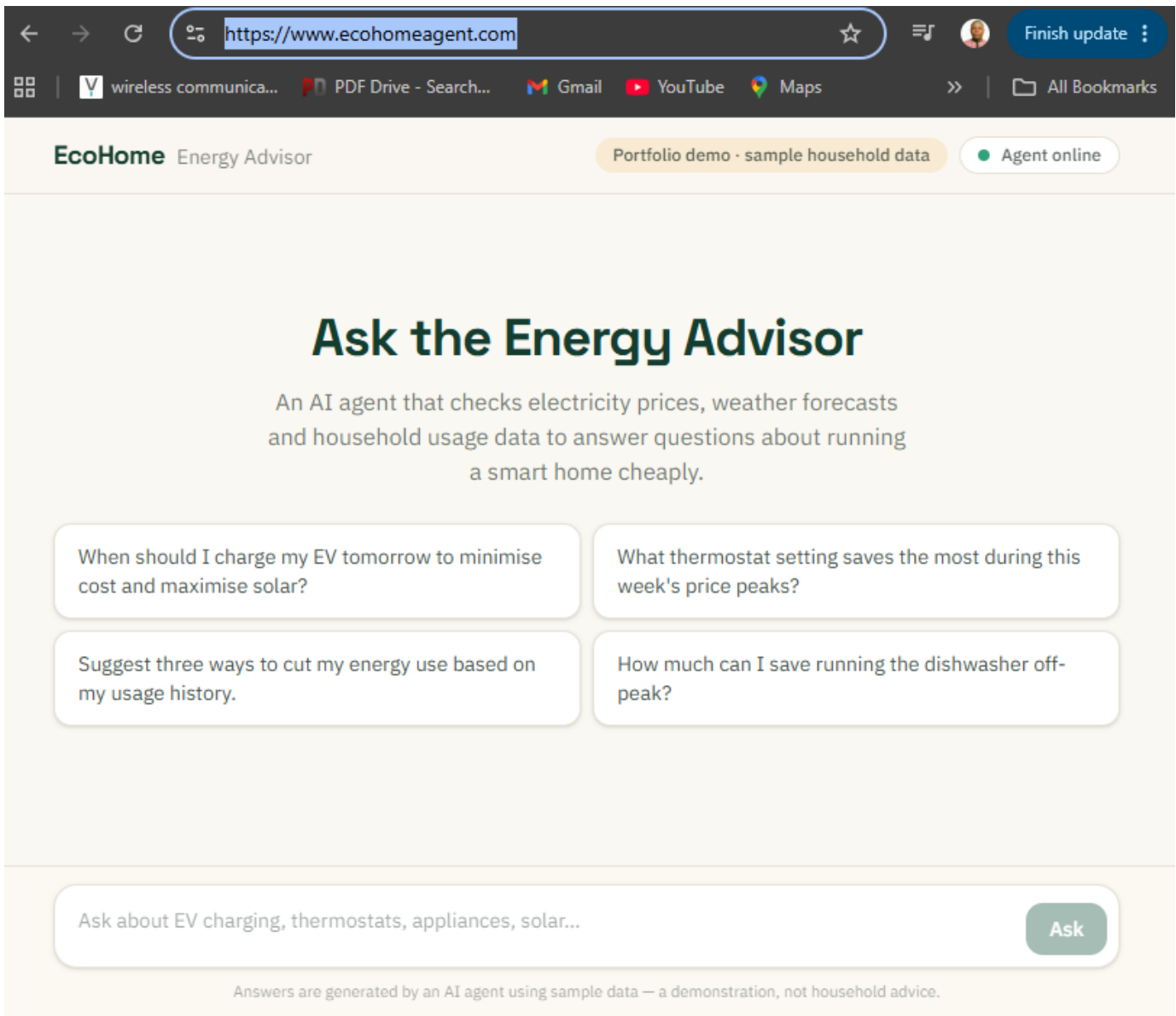


Fig. 7. Web interface of the EcoHome Energy Agent. The side panel shows the live Agile price profile and household usage and solar patterns. Example prompts illustrate supported request types. The response grounds a solar-aware recommendation in the forecast irradiance peak and the retrieved half-hourly prices.

- [37] L. Shu and D. Zhao, “Can AI make energy retrofit decisions? an evaluation of large language models,” 2025.
- [38] M. Giudici, A. Sironi, I. Villa, S. Scherini, and F. Garzotto, “Generating HomeAssistant automations using an LLM-based chatbot,” 2025.
- [39] D. Rivkin, F. Hogan, A. Feriani, A. Konar, A. Sigal, X. Liu, and G. Dudek, “Aiot smart home via autonomous llm agents,” *IEEE Internet of Things Journal*, vol. 12, no. 3, pp. 2458–2472, 2024.
- [40] T.-C. Li, Y.-K. Liu, and Y.-C. Tsai, “AI-driven smart home energy optimization: Integrating AI agents with IoT for adaptive decision-making,” in *IET Conference Proceedings*, 2025, pp. 225–230.
- [41] N. V. Gkalinikis, C. Nalmpantis, D. Vrakas, S. Chatzigeorgiou, C. Athanasiadis, and D. Doukas, “RHEA: Residential home energy advisor,” in *Proceedings of the 10th International Conference on Smart and Sustainable Technologies (SpliTech)*, 2025.
- [42] V. S. Raghavan and A. V. Giridhar, “Cost-optimal residential energy scheduling via a zero-shot LLM agent and model predictive control,” *Journal of Building Performance Simulation*, pp. 1–19, 2025.
- [43] Octopus Energy, “Agile octopus and the octopus energy API,” 2026, product AGILE-24-10-01; tariff E-1R-AGILE-24-10-01-C; region C. Accessed: 2026-07-05. [Online]. Available: <https://developer.octopus.energy/>
- [44] P. Zippenfenig, “Open-meteo.com weather API,” 2023. [Online]. Available: <https://doi.org/10.5281/zenodo.7970649>
- [45] Y. Liu *et al.*, “Prompt injection attack against LLM-integrated applications,” 2023.

**What thermostat setting saves the most during this week's price peaks?**

### Recommendation for Thermostat Setting During Price Peaks

**\*\*Optimal Setting:\*\*** Set your thermostat to **\*\*18°C\*\*** during peak hours (16:00 - 19:00) this week.

#### Cost Analysis:

- **\*\*Peak Hours (16:00 - 19:00):\*\***
- 16:00: £0.2155/kWh
- 17:00: £0.215/kWh
- 18:00: £0.2257/kWh
- **\*\*Total Cost for 3 hours at 18°C:\*\***
- If your HVAC system uses 1 kWh per hour, the cost would be approximately:
- 16:00: £0.2155
- 17:00: £0.215
- 18:00: £0.2257
- **\*\*Total:\*\*** £0.6562

#### Solar Consideration:

- **\*\*Solar Generation:\*\*** The forecast indicates low solar generation during peak hours due to cloudy conditions. Therefore, relying on solar power during these times is not feasible.

#### Savings Estimate:

- Since there is no historical HVAC usage data available for this week, I cannot provide a specific savings estimate. However, setting your thermostat to 18°C instead of a higher temperature (e.g., 20°C) can lead to significant savings, especially during peak pricing.

#### Reason for Recommendation:

- **\*\*Best Practice Tip:\*\*** Lowering your thermostat setting by just 1°C can lead to energy savings of about 10%. This is particularly important during peak pricing hours when electricity

Fig. 8. Thermostat scheduling interaction. The agent retrieves Agile prices, identifies the cheapest and most expensive hours, quantifies the per-kWh saving, and discloses the electricity price retrieval tool used beneath the response.